

## METHODS

**Mice.** Young (6–12 weeks) and old (22–30 months) wild-type C57BL/6 mice of both genders were either bred and aged in house, or purchased from the National Institute on Aging (NIA) aged rodent colonies. For transplantations experiments, 8–12-week-old CD45.1 C57BL/6-Boy/J recipient mice were lethally irradiated (11 Gy, delivered in split doses 3 h apart) and injected retro-orbitally with 250 to 5,000 purified CD45.2 HSCs delivered together with 300,000 Sca1-depleted helper CD45.1 bone marrow cells. Transplanted mice were kept on antibiotic-containing water for 4 weeks and analysed for donor-derived chimaerism by regular bleeding. Peripheral blood was obtained from retro-orbital bleeding, and collected in 4 ml of ACK (150 mM NH<sub>4</sub>Cl, 10 mM KHCO<sub>3</sub>) containing 10 mM EDTA for flow cytometry analyses. Cyclophosphamide (C)/granulocyte colony-stimulating factor (G-CSF) mobilization treatment was performed as previously described<sup>11</sup>. For mouse studies, no specific randomization or blinding protocol was used, and all experiments were performed in accordance with University of California San Francisco (UCSF) Institutional Animal Care and Use Committee approved protocols.

**Flow cytometry.** Enrichment and cell staining procedures for isolating HSCs (Lin<sup>-</sup>/c-Kit<sup>+</sup>/Sca1<sup>+</sup>/Flk2<sup>-</sup>/CD48<sup>-</sup>/CD150<sup>+</sup>), MPPs (Lin<sup>-</sup>/c-Kit<sup>+</sup>/Sca1<sup>+</sup>/Flk2<sup>+</sup>) and GMPs (Lin<sup>-</sup>/c-Kit<sup>+</sup>/Sca1<sup>-</sup>/CD34<sup>+</sup>/FcγR<sup>+</sup>) from c-Kit-enriched bone marrow, and granulocytes (Mac-1<sup>+</sup>/Gr-1<sup>+</sup>) from unfractionated bone marrow were performed as described<sup>29</sup>. In brief, HSCs were stained with un-conjugated lineage antibodies (Gr-1, Mac1, B220, CD3, CD4, CD5, CD8, Ter-119; all obtained from the UCSF Hybridoma Core Facility), goat anti-rat-PE-Cy5 (Invitrogen, A10691), c-Kit-APC-eFluor780 (eBioscience, 47-1171-82), Sca1-PB (BioLegend, 108120), Flk2-Bio (eBioscience, 13-1351-82), CD48-Alexa Fluor 647 (BioLegend, 103416), CD150-PE (BioLegend, 115904) and SA-PE-Cy7 (eBioscience, 25-4317-82) antibodies. FcγR-PerCP-eFluor710 (eBioscience, 46-0161-82) and CD34-FITC (eBioscience, 11-0341-85) were eventually included for concomitant isolation of MPPs and GMPs, and granulocytes were stained with Mac-1-PE-Cy7 (eBioscience, 25-0112-82) and Gr-1-PB (eBioscience, 57-5931-82) antibodies. CD45.1-FITC (eBioscience, 11-0454-85) was also included for isolation of donor-derived HSCs following transplantation. Blood chimaerism was analysed using CD45.2-FITC, eBioscience, 12-0453-83), B220-APC-e780 (47-0452-82), Gr-1-PB, Mac-1-PE-Cy7, CD3-e660 (eBioscience, 50-0032-82) and Ter-119-Cy5PE (eBioscience, 15-5921-83) antibodies. Stained cells were re-suspended for final analysis in Hanks buffered salt solution (HBSS) with 2% heat-inactivated fetal calf serum (FCS) and 1 μg ml<sup>-1</sup> propidium iodide (PI) for dead cell exclusion. For intracellular Ki67 and 4',6-diamidino-2-phenylindole (DAPI) staining, 5 × 10<sup>6</sup> unfractionated BM cells were surface stained for HSC markers as described earlier, fixed in Cytotfix/Cytoperm buffer (BD Biosciences, 554714) for 2 h at 4 °C, washed in PermWash (BD Biosciences), permeabilized with CytoPerm Plus (BD Biosciences) for 10 min at room temperature, re-fixed in Cytotfix/Cytoperm buffer for 10 min at 4 °C, washed in PermWash and stained with FITC-conjugated anti-Ki67 (Vector Laboratories) for 1 h at room temperature. Cells were washed in PermWash and resuspended in PBS/2% FCS. DAPI was subsequently added to samples and allowed to incubate for 20 min at room temperature before analysis. Cell isolation was performed on a FACS ARIAII (BD), using double sorting to ensure maximum purity, and cell analysis was performed on a FACS LSRII (BD).

**Cell culture.** All cell irradiation procedures were performed using a <sup>137</sup>Cs source (J. L. Shepherd & Associates Radiation Machinery, M38-1 S.N. 1098). Cells were cultured in Iscove's modified Dulbecco's media (IMDM) supplemented with 5% FBS (StemCell Technology, 06200), 1 × penicillin/streptomycin, 0.1 mM non-essential amino acids, 1 mM sodium pyruvate, 2 mM L-glutamine and 50 μM 2-mercaptoethanol (base media) and containing the following cytokines (all from PeproTech): IL-3 (10 ng ml<sup>-1</sup>), GM-CSF (10 ng ml<sup>-1</sup>), SCF (25 ng ml<sup>-1</sup>), IL-11 (25 ng ml<sup>-1</sup>), Flt-3L (25 ng ml<sup>-1</sup>), Tpo (25 ng ml<sup>-1</sup>) and Epo (4 U ml<sup>-1</sup>) (culture media). Aphidicolin (50 ng ml<sup>-1</sup>; Sigma, A4487), hydroxyurea (100 μM; Sigma, H8627), etoposide (0.25 μM; Sigma, E1383), staurosporine (5 nM; Sigma, S6942) or dimethylsulphoxide (DMSO) (vehicle) were added to the culture media as indicated. All cultures were performed at 37 °C in a 5% CO<sub>2</sub> water jacket incubator (Thermo Scientific). For DNase I treatment, cells were fixed with 4% PFA at room temperature, permeabilized in 0.2% Triton X-100 for 2 min at room temperature and incubated with 50 U of DNase I (Sigma, D4527) in 3% BSA, 5 mM MgCl<sub>2</sub>, 2 mM CaCl<sub>2</sub>, 0.2 × PBS for 10 min at 37 °C. For single-cell tracking experiments, cells were sorted directly into 96-well plates (1 cell per 100 μl per well, 96 wells scored per condition), visually inspected after 12 h to confirm successful single-cell sort, and, again, at the indicated time points to establish the kinetics of the first (appearance of 2 or more cells) and second (appearance of 4 or more cells) cell divisions. For EdU incorporation, cells were cultured for 16 h, pulsed for 1 h with 10 μM EdU (Life Technologies, C10339), harvested by 17 h and deposited onto poly-lysine coated slides (Thermo Scientific). For EdU/BrdU incorporation, cells were cultured for 16 h, pulsed for 1 h with 10 μM EdU, washed three times and incubated for 3 h in culture media without thymidine analogues, pulsed for 1 h with 60 μM BrdU (Sigma, B5002), harvested by 21 h and deposited onto poly-lysine-coated slides. For apoptosis assays, cells were sorted directly into

384-well solid white luminescence plates (400 cells per 40 μl per well, triplicate wells per condition) and analysed after 36 h culture by adding 40 μl of Caspase-Glo 3/7 (Promega) to each well, shaking at 300 r.p.m. for 30 s, incubating for 45 min at room temperature and reading on a luminometer (Synergy2, BioTek) to obtain relative luciferase units (RLU).

**Immunofluorescence staining.** Cells were either directly sorted or pipetted onto poly-lysine coated slides (500–2,000 cells per slide), incubated for 10 min, fixed with 4% PFA for 10 min at room temperature, permeabilized in 0.15% Triton X-100 for 2 min at room temperature and blocked in 1% BSA/PBS overnight at 4 °C. Slides were then incubated for 1 to 2 h at 37 °C in 1% BSA/PBS with the following antibodies alone or in combination: anti-phospho-H2AX (Ser 139) (Millipore, 05-636), anti-53BP1 (Novus Biologicals, NB100-904), anti-phospho-CHK1 (Ser 345) (Cell Signaling, 2348), anti-phospho-ATM (Ser 1981) (Active Motif, 39529), anti-PAR (BD Pharmingen, 550781), anti-RPA (70 kDa) (Thermo Scientific, PA5-21976), anti-ATRIP (Thermo Scientific, PA1-519), anti-MCM4 and anti-MCM6 (provided by J.M.), anti-FBL (Cell Signaling, 2639), anti-UBF (gift from B. McStay), anti-NCL (Abcam, ab22758), anti-NPM1 (Invitrogen, 32-5200), anti-PP4C (Bethyl Laboratories, A300-835A), anti-CENP-A (Cell Signaling, 2048), anti-H3K9me3 (Abcam, 8898), anti-H3K27me3 (Millipore, 07-449), anti-H3K4me3 (Invitrogen, 49-1005) and anti-H3K79me2 (Abcam, ab3594). Slides were washed three times in PBS and incubated for 1 h at 37 °C in PBS/1% BSA with appropriate secondary antibodies (all from Life Technologies): A488-conjugated goat anti-mouse (A-11029), A594-conjugated goat anti-rabbit (A-11037), A594-conjugated donkey anti-sheep (A-11016) and A488-conjugated donkey anti-mouse (A-21202). Slides were then washed three times in PBS and mounted using VectaShield (Vector Laboratories) containing 1 μg ml<sup>-1</sup> DAPI. For γH2AX/PNA immuno-FISH staining, cells were re-fixed with 4% PFA for 5 min after γH2AX staining and then processed for FISH as previously described<sup>30</sup>. For γH2AX/rDNA immuno-FISH staining, cells were first fixed with ice-cold methanol for 2 min before blocking, then re-fixed with 2% PFA for 5 min after γH2AX staining and processed for FISH according to the manufacturer's recommendations (FISHTag DNA kit, Molecular Probes, F32949), with a 3 h RNase treatment step at 37 °C replacing the suggested HCl/pepsin treatment before dehydration of the slides. The rDNA FISH probe corresponded to a 11.35 kb EcoRI-EcoRI fragment of the pMr974 mouse rDNA plasmid comprising parts of the non-transcribed spacer, the 50 external transcribed spacer and the majority of the 18S sequence (gift from I. Grumt). TUNEL staining was performed according to the manufacturer's recommendations (Roche, 11684795910). EdU incorporation was detected using A594-labelled azide click chemistry according to the manufacturer's instruction (Life Technologies, Click-iT EdU imaging assay, C10339). For EdU/BrdU double labelling, cells were re-fixed with 3.7% PFA for 5 min after EdU labelling, denatured with 2 N hydrochloric acid for 30 min at room temperature, washed with borate buffer (100 mM, pH 8.5) for 10 min, and incubated with A488-conjugated anti-BrdU (Life Technologies, B35130) overnight at 4 °C. For EdU/γH2AX double staining, cells were re-fixed with 4% PFA for 5 min after EdU labelling and stained for γH2AX. Images were acquired on a SP5 Leica Upright Confocal Microscope (×10, ×20 or ×63 objective) and processed using the Velocity software (Perkin Elmer v.6.2). A (mean DAPI intensity × nuclear area) cut-off of ≤1,100 was used to identify G1-phase cells in 36 h culture. An average of 150 cells (EdU and EdU/BrdU incorporation assays, persistent G1-phase 53BP1 bodies), 200 cells (γH2AX quantification) and 30 cells (all other immunofluorescence analyses) were scored from at least two independent experiments.

**Single-molecule DNA replication analyses.** Replication track analyses were adapted from a published protocol<sup>31</sup>. In brief, cells were cultured for 36 h, pulsed for 38 min with 50 μM CldU (Sigma, C6891), washed twice with IMDM base media, pulsed for 38 min with 250 μM IdU (Sigma, I7125), washed once with IMDM base media, spotted onto glass slides and lysed for 36 min with 10 μl of spreading buffer (0.5% SDS in 200 mM Tris-HCl (pH 7.4) and 50 mM EDTA). Slides were tilted at a 15° angle to allow DNA to spread, fixed in 3:1 volume absolute methanol:glacial acetic acid for 2 min and air-dried. DNA was denatured with 2.5 M HCl for 30 min at room temperature, and slides were rinsed three times in PBS and blocked in PBS/0.1% Triton X-100/1% BSA for 1 h at room temperature. Cells were incubated for 1 h at room temperature with rat anti-BrdU (Abcam, ab6326) and mouse anti-BrdU (Becton Dickinson, 347580) antibodies to detect CldU and IdU, respectively, together with a mouse anti-single-stranded DNA antibody (Millipore, MAB3034) to check for DNA fibre integrity. Slides were washed three times in PBS and incubated for 30 min at room temperature with A488-conjugated goat anti-mouse (Molecular Probes, A-21121), A594-conjugated goat anti-rat (Life Technologies, A-11007) and A647-conjugated anti-mouse IgG2a (Molecular Probes, A-21241) secondary antibodies. Slides were then washed three times in PBS and mounted in Prolong Plus (Invitrogen, P36930). Tracks were imaged on a DM6000 B Leica microscope and fork rate (FR) was calculated based on the length of the IdU tracks measured using ImageJ software and the following formula: FR (kb min<sup>-1</sup>) = ((2.59 (kb μm<sup>-1</sup>) × length (μm)) /

pulse time (min)). At least 300 replication tracks were analysed per experiment, and 100 origins were used to calculate fork symmetry ratios.

**Gene expression.** Total RNA was isolated from  $1-2 \times 10^4$  cells sorted directly into TRIzol-LS (Invitrogen) according to the manufacturer's protocol. Bioanalyzer chips were used to control for RNA quality and quantify RNA by dividing the area under the curve by the total cell number. For qRT-PCR, RNA was treated with DNase I and reverse-transcribed using SuperScript III kit and random hexamers (Invitrogen). Runs were performed on a 7900HT Fast Real-Time PCR System (Applied Biosystems) using SYBR Green reagents (Applied Biosystems) and the cDNA equivalent of 200 cells per reaction. Sequences for qRT-PCR primers were: *Ccna2*, forward, CAGCA TGAGGGCGATCCTT; reverse, GCAGGGTCTCATTCTGTAGTTTATATTCT (NM\_009828); *Ccnb2*, forward, GCATCATGCGACGGTTCCT; reverse, TCCCG ACCACCTGCAGTTT (NM\_172301); *Ccnd1*, forward, TGTTACTGTAGCGG CCTGTTG; reverse, CCGGAGACTCAGAGCAAATCC (NM\_007631); *Ccne1*, forward, GCAGCGAGCAGGAGACAGA; reverse, GCTGCTTCCACACCCT GTCTT (NM\_007633); *Cdc6*, forward, CTACCTTTCTGGCGCTCCT; reverse, GGATTTAAAGCCTTTACTTCTCTC (NM\_011799.2); *Cdc45*, forward, AGT TCCTGGAGCTCTTGTG; reverse, GGAAAAGGAGGTCACTTCTGG (NM\_009862.2); *Cdkn1a*, forward, TTCCGCACAGGAGCAAAGT; reverse, CGGCGC AACTGCTCACT (NM\_007669); *Cdkn1c*, forward, CAGCGGACGATGGAAGA ACT; reverse, CTCCGGTTCCTGTACATGAA (NM\_009876); *Cdkn2a*, forward, CCCAAGCCCGCAACT; reverse, GTGAACGTTGCCCATCATCA (NM\_001 040654); *Gins1*, forward, ATGAGGACGGACTCAGACAAG; reverse, TCCAGC TGACTTGGCTTCAT (NM\_027014.1); *Gins2*, forward, CGGAATGGATGGAT GTGG; reverse, GGCAGTGGGGTGAATGTC (NM\_178856.1); *Gins3*, forward, ACAGTCCGGAGAATGCAGAT; reverse, GCGGAACCGTCCAATAAAA (NM\_030198.3); *Gins4*, forward, CCTAATCTCTGCAGAGTCATT; reverse, AGGG GCAAACCTTTCATTCA (NM\_024240.6); *Mcm2*, forward, AGAAGTTCAGC GTCATGCGGAGTA; reverse, CCCAAAGCGGTTGCGTTGATATGT (NM\_00 8564.2); *Mcm3*, forward, AGGAAGACTCATGCCAAGGATGGA; reverse, TGG GTCCTACTGAGTTCACCTTCT (NM\_008563.2); *Mcm4*, forward, ACAGGAA TGAGTGGCACTTCTCGT; reverse, AAAGCTCGACGGCTTCTTCAAAC (NM\_008565.3); *Mcm5*, forward, CTGGATGCTGCTTGTCTGGCAAT; reverse, TG TGTTACAGACCTGAGAGCCAA (NM\_008566.2); *Mcm6*, forward, GGACC AAGTTGCTATTCA; reverse, ATTCAGAGTTGCCCTCAC (NM\_008567.1); *Mcm7*, forward, CCCTGCCCAATTTGAACCTTTGGA; reverse, TCTCCACATATGC TGCCGTGATGT (NM\_008568.2); *Prkdc*, forward, GCCATGAGCTTAGGTT TCAAT; reverse, CTAAGAGCTTTCAGCAGGTTTCA (NM\_011159.2); *Rad51*, forward, AAGTTTTGGTCCACAGCCTATTTT; reverse, CGGTGCATAAGCAAC AGCC (NM\_011234.4); *Rad54*, forward, CCAAGTCCAGGAGTGTTCCT; reverse, GGCCGGTTGAGTAGTCTGAGT (NM\_009015.3); *Rpa1*, forward, ACATCCGT CCCATTCTACAGG; reverse, CTCCTCGACCAGGGTGT (NM\_026653.1); *Xrcc2*, forward, GGAAGGCCACATGTGAGT; reverse, GGATCGTTTGTG ACATAGGCATT (NM\_020570.2); *Xrcc3*, forward, CCTGAGGAGCTGATCG AGAAGA; reverse, CGGCCGCGTGTCAAT (NM\_028875.2); *Xrcc5*, forward, GACTTGGCGCAATACATGTTTTT; reverse, AAGCTCATGGAATCAATCA GATCA (NM\_009533); *Xrcc6*, forward, GGAGTCAAGCAAGTGGAAAG; reverse, AGAACTCGCTTTTTGGTCTCCTT (NM\_010247.2); *47S rRNA*, forward, CT CTTAGATCGATGTGGTGCTC; reverse, GCCCGCTGGCAGAACGAGAAG (BK000964); *53bp1*, forward, TACAGCCCGGTAAAGGTATCCAT; reverse, CT GGACGGCCGGTCTT (NM\_013735.3); *Actb*, forward, GACGGCCAGGTCA TCACTATTG; reverse, AGGAAGCTGAAAAGAGCC (NM\_007393). Values were normalized to *Actb* expression. For microarray analyses, RNA was purified using Arcturus PicoPure (Applied Biosystems) with RNase-free DNase (Qiagen), amplified, labelled, and fragmented using NuGEN Ovation Pico linear amplification kits (Nugen Technologies) and hybridized onto mouse Gene ST 1.0 arrays (Affymetrix). Microarray data were analysed using the limma package (v. 3.12.3) for the R programming language (v. 2.15.1) and fitted with a zero-intercept linear model with age (young versus old) and cell type (HSCs versus GMPs) as coefficients<sup>32</sup>. Genes that were significantly differentially expressed between young and old HSCs, but not between young and old GMPs, were extracted and submitted to hierarchical clustering with Euclidean distance and Ward's linkage. Four clusters of genes were defined and analysed with conditional GO-term enrichment using the GOSTATS package (v. 2.22.0) (Supplementary Table 2). Published data sets for genes differentially expressed in young and old HSCs (gene expression omnibus (GEO) accession numbers GSE27686, GSE39553, GSE6503, GSE32719)<sup>3,4,33,34</sup> were re-analysed as follows. Each data set was normalized using Robust Multi-Array Average (RMA)

as implemented in the Affymetrix package for the R programming language. Expression measurements for probes mapping to *Mcm* genes were used in a non-supervised hierarchical clustering using Euclidean distance and Ward's linkage and plotted as a heatmap.

**Lentiviral transduction.** Lentiviral-mediated transduction experiments were performed as described<sup>35</sup>. Briefly, pGFP-C-shLenti vectors containing shRNA targeting murine *Mcm4* (TL514127) and *Mcm6* (TL510769) genes or non-targeting scrambled shRNA (TR30021) were purchased from Origene. Four independent shRNA constructs were purchased and tested for each gene. Lentiviral supernatants were produced by the UCSF Lentiviral Core Facility with titres ranging from  $2.2$  to  $4.3 \times 10^8$  infectious particles per ml. Cells were left to recover in IMDM base media for 1–2 h post-sort and spin-infected for 90 min (2,000g, 37 °C) with 1:25 dilution of lentiviral supernatants. After 3 h recovery at 37 °C in a 5% CO<sub>2</sub> water jacket incubator, the medium was replaced with cytokine-containing IMDM culture media and cells were cultured for 48 h before re-isolation of live PI<sup>-</sup>/GFP<sup>+</sup> transduced cells for *in vitro* experiments, or for 12 h for transplantation experiments.

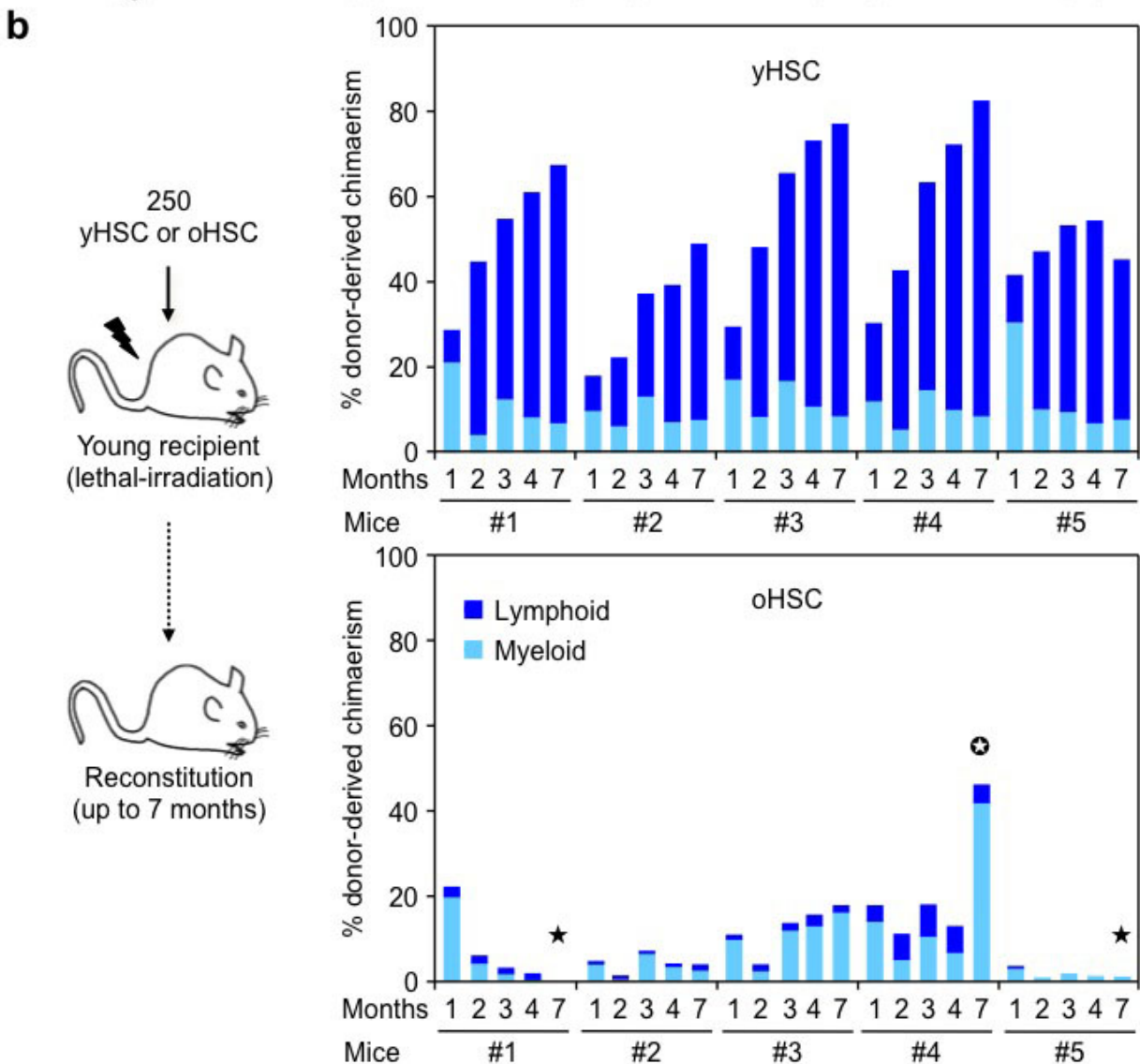
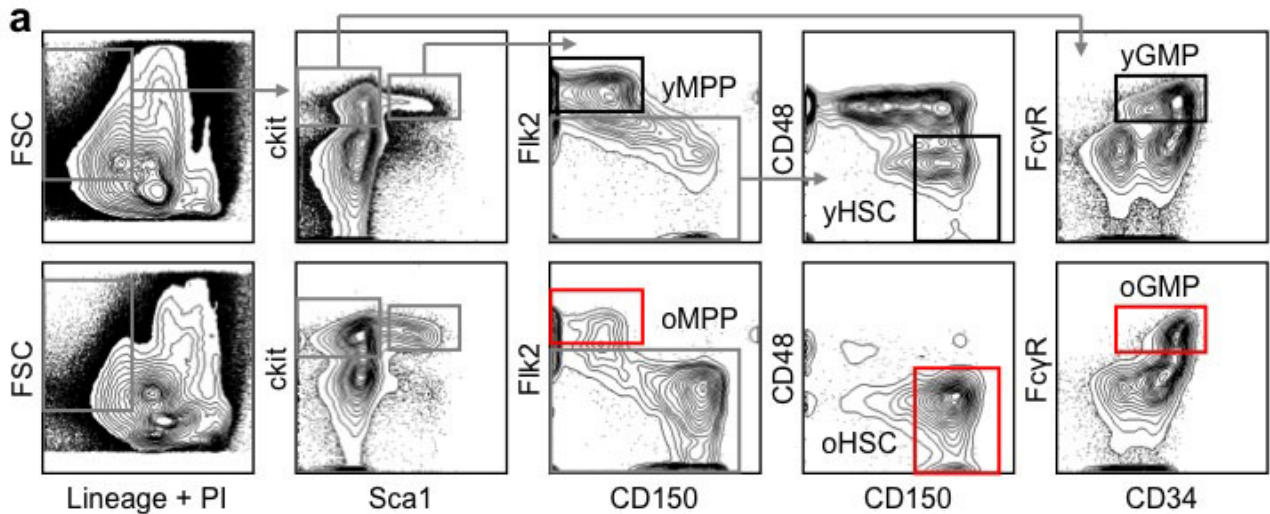
**Comet assay.** Alkaline comet assays were performed as described<sup>36</sup>. Briefly,  $8 \times 10^3$  cells diluted in 0.4 ml of PBS were added to 1.2 ml of 1% low-gelling-temperature agarose (Sigma) and transferred onto slides also pre-coated with 1% low-gelling-temperature agarose. Cells were lysed in alkaline lysis solution (1.2 M NaCl, 100 mM Na<sub>2</sub>EDTA, 0.1% sodium lauryl sarcosinate, 0.26 M NaOH (pH >13)) overnight at 4 °C. Slides were then washed three times with electrophoresis buffer (0.03 M NaOH, 2 mM Na<sub>2</sub>EDTA (pH ~12.3), and run for 25 min at 0.6 V cm<sup>-1</sup>. Nuclei were stained with 2.5 µg ml<sup>-1</sup> PI in distilled water for 20 min. Pictures of individual cells were taken with a Leica confocal inverted microscope (×10 objective, gain 1) and analysed using the CASP software (<http://casplab.com/>). The tail moment of all comets analysed was used to define outliers and non-outliers based on calculated absolute deviation. Cells were defined as outliers when their tail moment absolute deviation was  $\geq 3$  median absolute deviation (MAD).

**Cytogenetic analyses.** For metaphase preparation, HSCs were cultured for 5 days, treated for 4 h with 0.01 µg ml<sup>-1</sup> Colcemid (Invitrogen), collected in Eppendorf tubes, washed once with PBS, incubated for 8 min at 37 °C in 0.075 M KCl and then fixed in 3:1 volume absolute methanol:glacial acetic acid. Metaphases were analysed by Giemsa staining and spectral karyotyping (SKY) as previously described<sup>11</sup>, or using the Metasystem's 21Xmouse probe cocktail and ISIS software for multi-color FISH (M-FISH) according to the manufacturer's instruction (MetaSystems). An average of 10 to 20 cells were scored per experiment.

**Cell biology assays.** Standard transmission electron microscopy ultrastructural analyses were performed as previously described<sup>29</sup>. β-Galactosidase activity was measured using the Senescence β-Galactosidase Staining Kit according to the manufacturer's instruction (Cell Signaling, 9860).

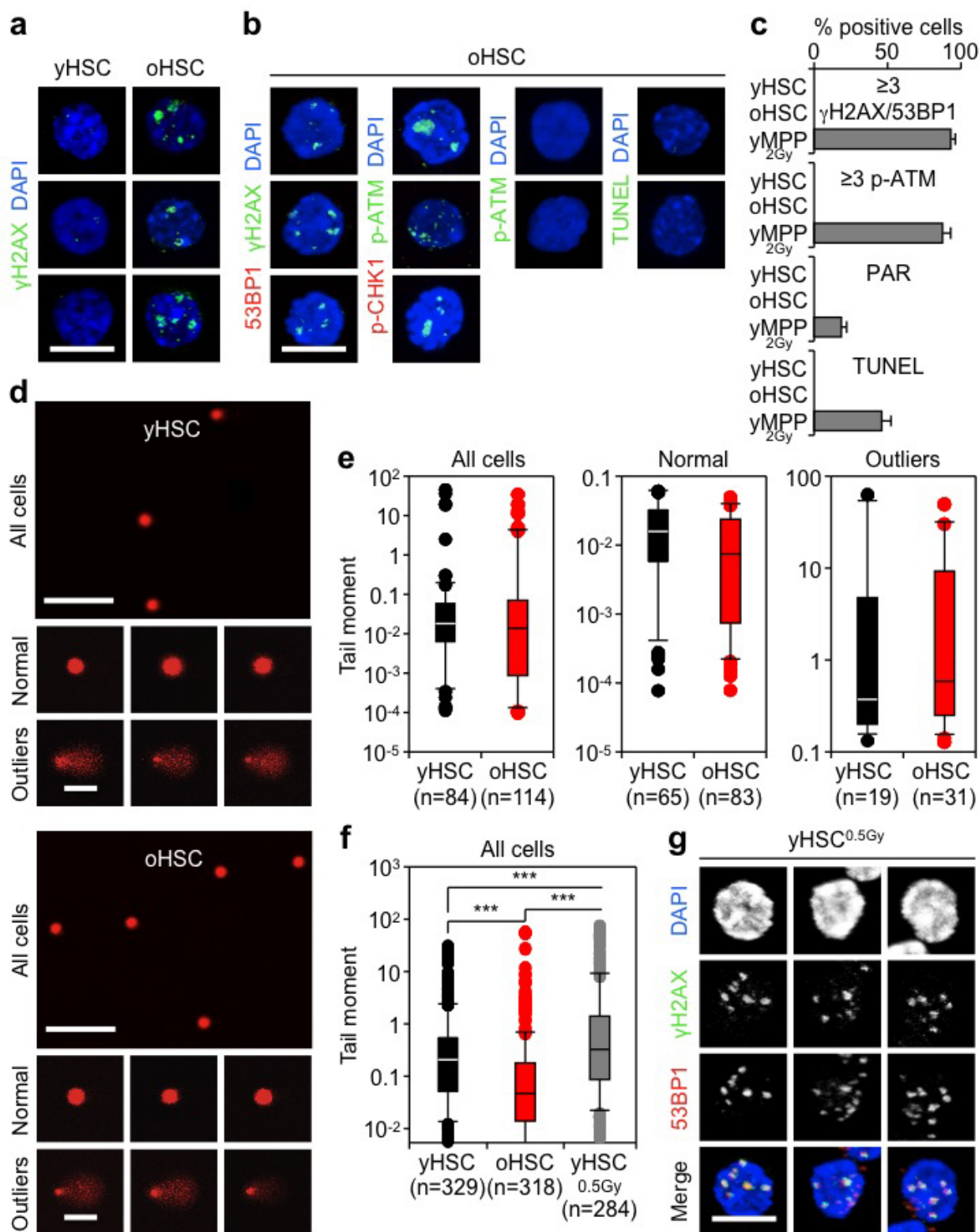
**Statistics.** Data were expressed as mean ± s.d. and *P* values were calculated using a two-tailed Student's *t*-test, unless indicated. No specific randomization or blinding protocol was used. For tail moments in comet assays, data were expressed as boxplots with whiskers and *P* values were calculated pairwise using the Mann–Whitney rank sum test. The Mann–Whitney rank sum test was also used to calculate statistical significance for replication track analyses. For microarray results, data were expressed as boxplots with whiskers and *P* values were calculated using a two-sided *t*-test. *P* values were considered significant when  $\leq 0.05$ . *N* indicates the numbers of independent experiments performed and was chosen to ensure adequate statistical power.

29. Warr, M. R. *et al.* FoxO3a directs a protective autophagy program in hematopoietic stem cells. *Nature* **494**, 323–327 (2013).
30. Cooley, C. *et al.* Trf1 is not required for proliferation or functional telomere maintenance in chicken DT40 cells. *Mol. Biol. Cell* **20**, 2563–2571 (2009).
31. Terret, M. E., Sherwood, R., Rahman, S., Qin, J. & Jallepalli, P. V. Cohesin acetylation speeds the replication fork. *Nature* **462**, 231–234 (2009).
32. Smyth, G. K. Linear models and empirical bayes methods for assessing differential expression in microarray experiments. *Stat. Appl. Genet. Mol. Biol.* **3**, Article 3 (2004).
33. Norddahl, G. L. *et al.* Accumulating mitochondrial DNA mutations drive premature hematopoietic aging phenotypes distinct from physiological stem cell aging. *Cell Stem Cell* **8**, 499–510 (2011).
34. Bersenev, A. *et al.* Lnk deficiency partially mitigates hematopoietic stem cell aging. *Aging Cell* **11**, 949–959 (2012).
35. Will, B. *et al.* Satb1 regulates the self-renewal of hematopoietic stem cells by promoting quiescence and repressing differentiation commitment. *Nature Immunol.* **14**, 437–445 (2013).
36. Olive, P. L. & Banath, J. P. The comet assay: a method to measure DNA damage in individual cells. *Nature Protocols* **1**, 23–29 (2006).



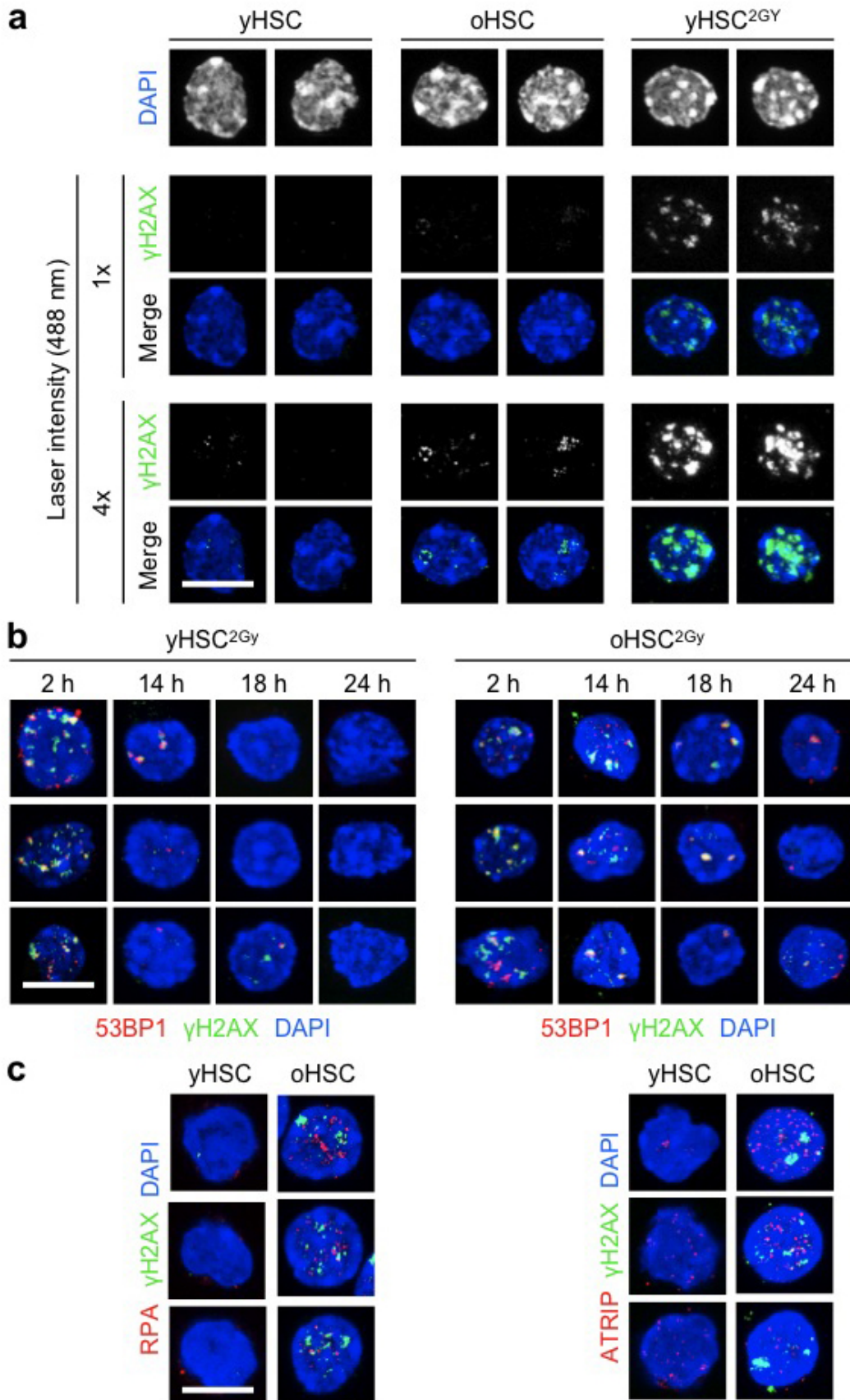
**Extended Data Figure 1 | Isolation strategy and functional impairment of old HSCs.** **a**, Gating strategy used to isolate HSCs ( $\text{Lin}^-/\text{Sca1}^+/\text{c-Kit}^+/\text{Flk2}^-/\text{CD150}^+/\text{CD48}^-$ ), MPPs ( $\text{Lin}^-/\text{Sca1}^+/\text{c-Kit}^+/\text{Flk2}^+$ ) and GMPs ( $\text{Lin}^-/\text{Sca1}^-/\text{c-Kit}^+/\text{Fc}\gamma\text{R}^+/\text{CD34}^+$ ) from the bone marrow of young (6–12 weeks) and old (22–30 months) C57BL/6 mice. o, old; y, young. **b**, Reconstitution ability of young and old HSCs. HSCs were isolated from C57BL/6-CD45.2 donor mice, and transplanted (250 HSCs per mouse) into lethally irradiated

young C57BL/6-CD45.1 recipients ( $n = 5$  mice per cell type) together with 300,000 Sca1-depleted CD45.1 helper bone marrow cells. The percentage of donor-derived chimaerism and myeloid (light blue) versus lymphoid (dark blue) reconstitution in the peripheral blood was assessed by flow cytometry at the indicated months post-transplantation. Stars indicate phenotypes resembling age-related blood disorders: black, bone marrow failure; white, myeloproliferative neoplasm.



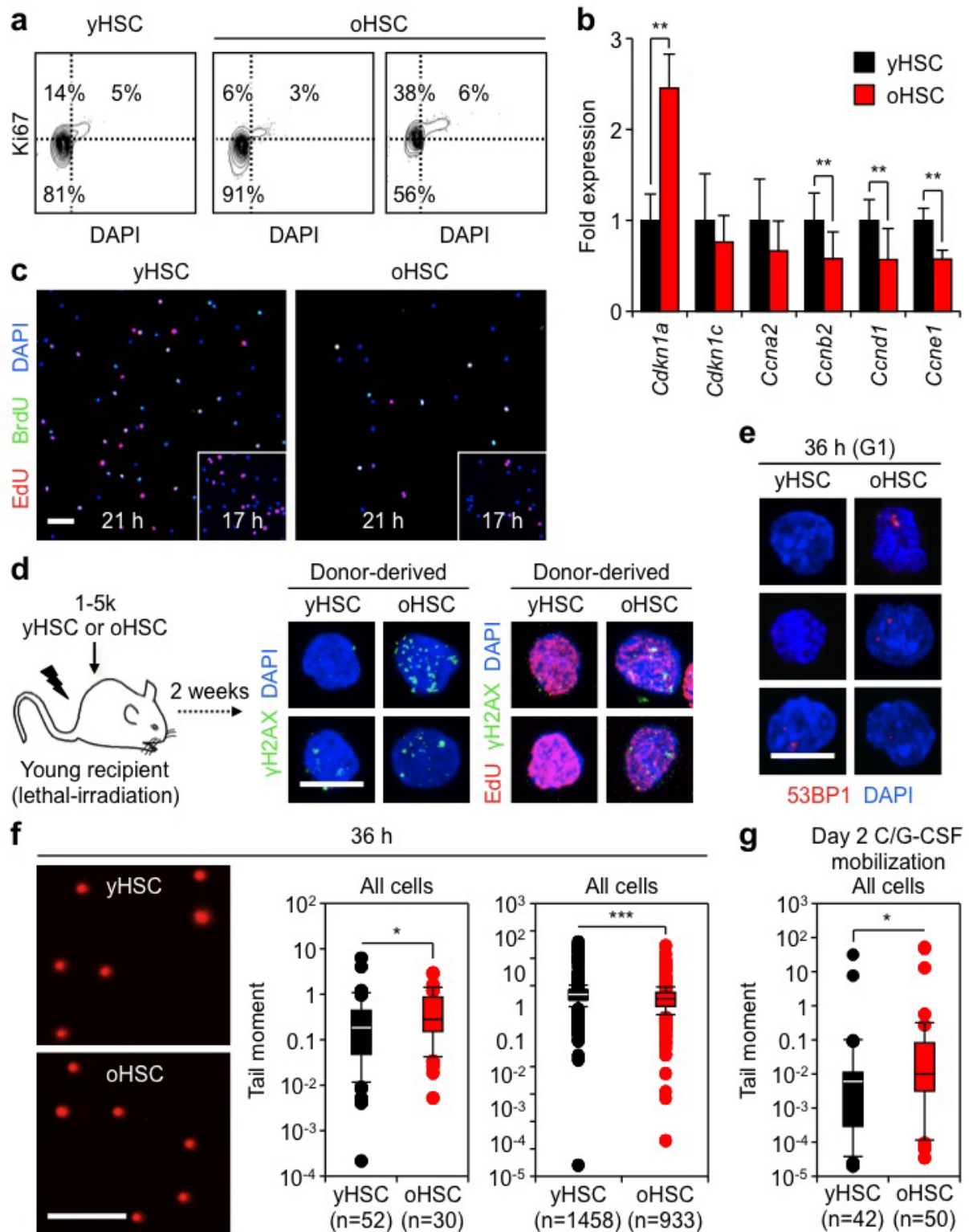
**Extended Data Figure 2 | Age-associated  $\gamma$ H2AX signals are not associated with markers of DNA damage.** **a**, Additional images for  $\gamma$ H2AX staining in young and old HSCs. **b**, Additional images for DNA damage markers in old HSCs. **c**, Quantification of DNA damage marker staining shown in Fig. 1c. **d**, Results are expressed as per cent of positive cells. **d**, Representative images of young and old HSCs analysed by alkaline comet assay showing a field view of all cells and examples of normal ( $< 3$  MAD) and outliers ( $\geq 3$  MAD) cells. MAD, median absolute deviation in mean tail moment. **e**, Mean tail moment

for young and old HSCs in one representative alkaline comet experiment. Results are expressed as boxplots with the line marking the median, the box the boundaries of the 25th and 75th percentiles, and the whiskers the 90th and 10th percentiles. **f**, Mean tail moment for young and old HSCs compared with 0.5 Gy irradiated young HSCs analysed by alkaline comet assay. Results are expressed as boxplots as in **e**.  $***P \leq 0.001$  (pairwise Mann–Whitney rank sum test). **g**, Representative images of  $\gamma$ H2AX/53BP1 foci in 0.5 Gy irradiated young HSCs. Scale bars, 10  $\mu$ m (**a**, **b**, **g**); 90  $\mu$ m (magnified cells, 60  $\mu$ m) (**d**).



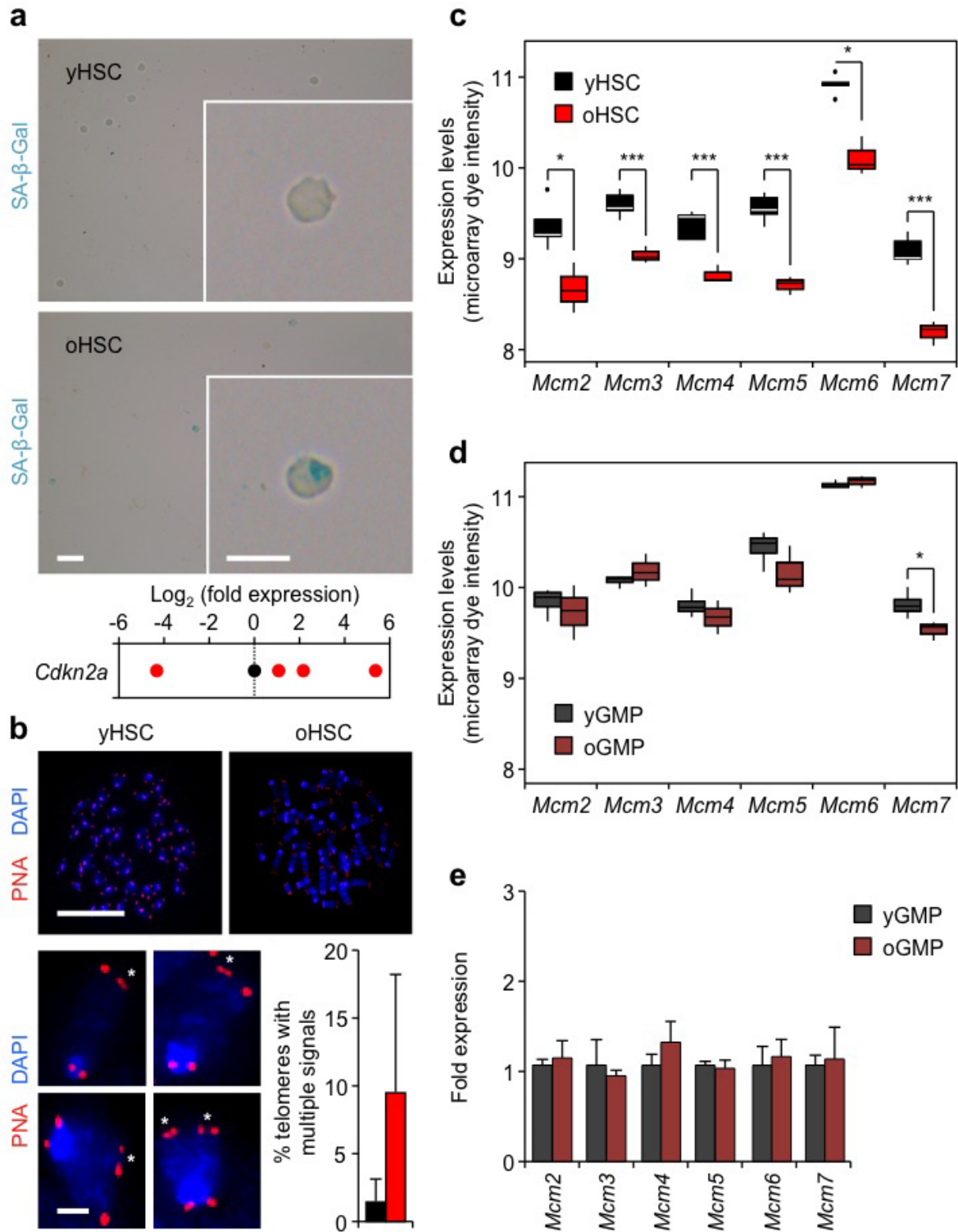
**Extended Data Figure 3 | Signal intensity, repair kinetics and residual replication stress in old HSCs.** a, Representative images comparing  $\gamma$ H2AX signal intensity in unirradiated young and old HSCs, and 2 Gy irradiated young HSCs. Two different intensity settings for the 488 nm laser are used.

b, Additional images for the clearance of  $\gamma$ H2AX/53BP1 foci in 2 Gy irradiated young and old HSCs. c, Additional images for  $\gamma$ H2AX/RPA and  $\gamma$ H2AX/ATRIP staining in young and old HSCs. Scale bars, 10  $\mu$ m.



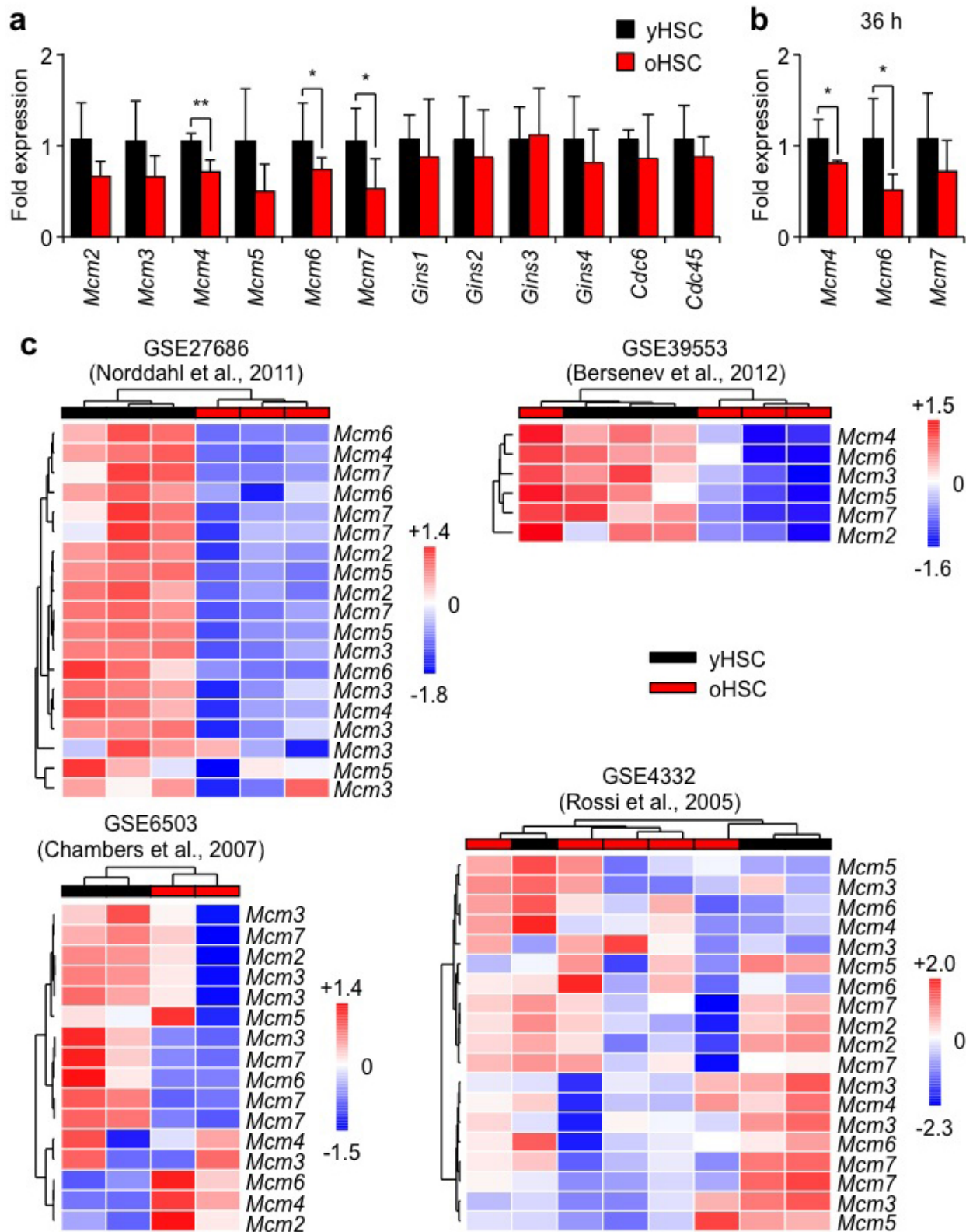
**Extended Data Figure 4 | Consequences of replication stress in cycling old HSCs.** **a**, Representative FACS plots for Ki67/DAPI intracellular staining in young and old HSCs. Two independent examples of old HSC staining are shown. **b**, qRT-PCR analyses of cell cycle gene expression in young and old HSCs ( $n = 5$ ). Results are expressed as fold change compared with young HSCs (set to 1). Data are means  $\pm$  s.d.  $**P \leq 0.01$ . **c**, Representative images of 17 h single EdU (insert) and 21 h double EdU/BrdU labelling experiments. **d**, Schematic and representative images of  $\gamma$ H2AX and  $\gamma$ H2AX/EdU staining in cycling young and old HSCs re-isolated 2 weeks after transplantation. **e**, Additional images of persistent 53BP1 bodies in 36 h cycling young and old HSCs that have re-entered G1 following replication. G1-phase cells were

identified as cells with mean DAPI intensity  $\times$  area  $\leq 11,000$ , and represented  $\sim 49\%$  (young HSCs) and  $\sim 52\%$  (old HSCs) of the population at that time. **f**, Representative field images and mean tail moment for 36 h cycling young and old HSCs analysed by alkaline comet assay. Results are expressed as boxplots with the line marking the median, the box the boundaries of the 25th and 75th percentiles, and the whiskers the 90th and 10th percentiles. Two independent examples of comet assays are shown. **g**, Mean tail moment for day 2 cyclophosphamide (C)/G-CSF mobilized young and old HSCs analysed by alkaline comet assay. Results are expressed as boxplots as in **f**.  $*P \leq 0.05$ ,  $***P \leq 0.001$  (pairwise Mann-Whitney rank sum test). Scale bars, 100  $\mu\text{m}$  (**c**); 10  $\mu\text{m}$  (**d**, **e**); 90  $\mu\text{m}$  (**f**).



**Extended Data Figure 5 | Rare cases of exacerbated replication stress and identification of MCM defect in old HSCs.** **a**, Representative images of senescence-associated  $\beta$ -galactosidase (SA- $\beta$ -Gal) staining and qRT-PCR analyses of *Cdkn2a* (p16) expression levels in young and old HSCs. Results are expressed as log<sub>2</sub> fold changes compared with young HSCs (set to 0). Only 2 out of 10 preparations of old HSCs showed SA- $\beta$ -Gal staining, while only 2 out of 9 preparations of young HSCs and 4 out of 12 preparations of old HSCs had detectable p16 levels. Of note, old HSCs with the highest p16 levels also scored positive for SA- $\beta$ -Gal staining. **b**, Representative images of telomere FISH on metaphase spreads of young and old HSCs. Magnified inserts show detection of multiple telomeric signals (asterisks) in old HSCs, and histograms indicate the per cent of all telomeres with multiple telomeric signals per young and old

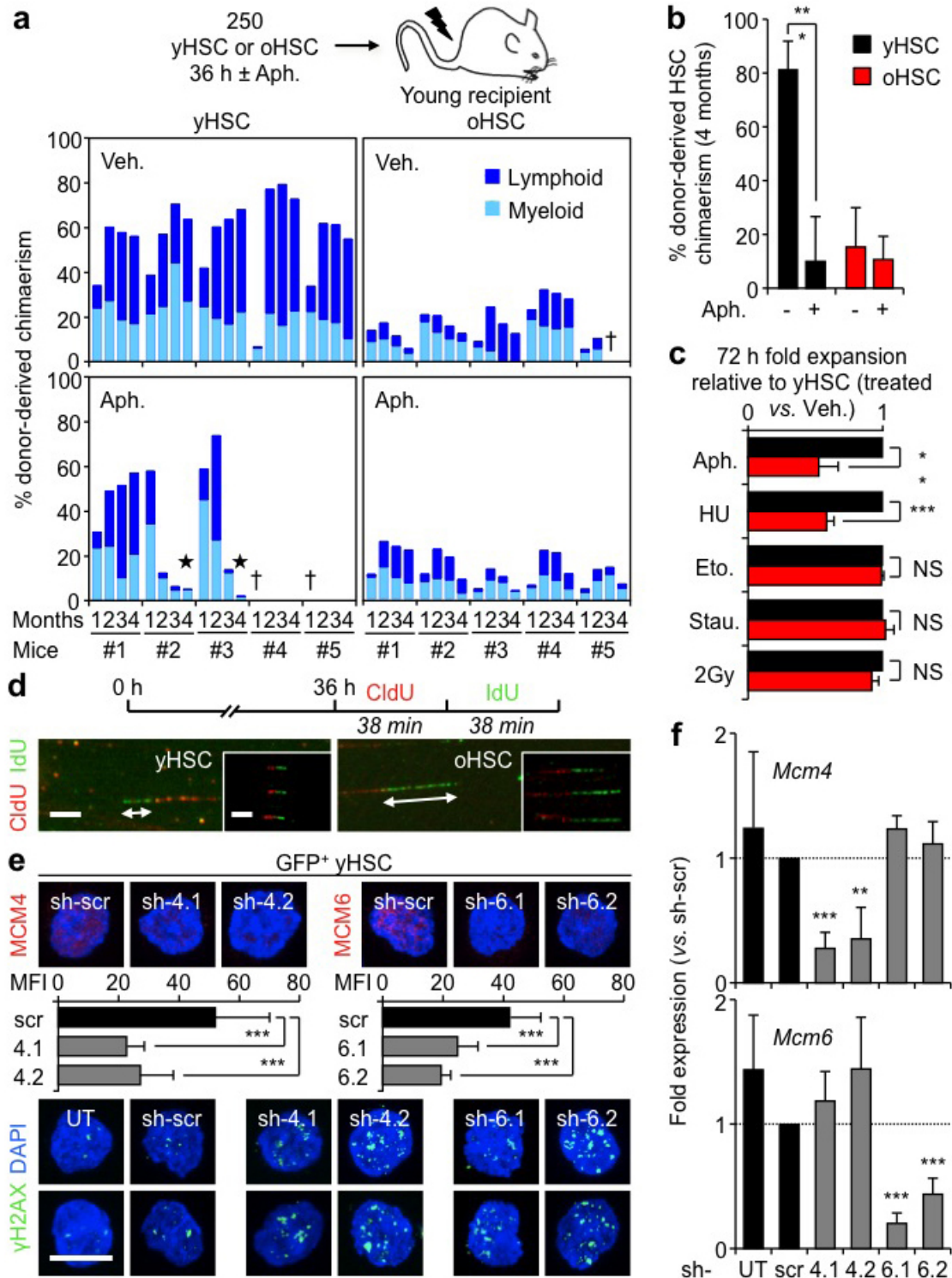
HSCs (7 and 6 cells scored, respectively). Only 2 out of 6 preparations of old HSCs showed multiple telomeric signals. Data are means  $\pm$  s.d. **c**, **d**, Microarray analysis showing differential *Mcm* gene expression in young and old HSCs (**c**) and GMPs (**d**). A total of 5 (young) and 3 (old) independent biological replicates were used for HSCs, and 4 (young) and 3 (old) for GMPs. Results are expressed as boxplots with the line marking the median, the box the boundaries of the 25th and 75th percentiles and the whiskers the  $\pm 1.5$  interquartile range. \* $P \leq 0.05$ , \*\* $P \leq 0.01$ , \*\*\* $P \leq 0.001$  (two-sided *t*-test). **e**, qRT-PCR analyses of *Mcm* gene expression in young and old GMPs ( $n = 3-5$ ). Results are expressed as fold change compared with young GMPs (set to 1). Data are means  $\pm$  s.d. Scale bars, 100  $\mu$ m; insert, 10  $\mu$ m (**a**); 10  $\mu$ m; magnified cells, 1  $\mu$ m (**b**).



**Extended Data Figure 6 | Specific decrease in *Mcm* gene expression in old HSCs.** **a, b**, qRT-PCR analyses of the expression of *Mcm* genes and other components of the pre-replication complex in quiescent (**a**) and cycling (**b**) young and old HSCs ( $n = 4-5$ ). Results are expressed as fold change compared with young HSCs (set to 1). Data are means  $\pm$  s.d. \* $P \leq 0.05$ , \*\* $P \leq 0.01$ . **c**, Re-analyses of published data sets for *Mcm* gene expression in old HSCs. Data from GEO accession number GSE27686 (ref. 33): HSCs were defined as  $\text{Lin}^-/\text{c-Kit}^+/\text{Sca1}^+/\text{CD34}^-/\text{CD150}^+$  with 3 young (10–12 weeks) and 3 old (100 weeks) samples. Data from GEO accession GSE39553 (ref. 34): HSCs were

defined as  $\text{Lin}^-/\text{c-Kit}^+/\text{Sca1}^+/\text{CD48}^-/\text{CD150}^+$  with 3 young (2 months) and 4 old (20 months) samples. Data from GEO accession number GSE6503 (ref. 4): HSCs were defined as  $\text{Lin}^-/\text{c-Kit}^+/\text{Sca1}^+/\text{Hoechst-33342}^{\text{low}}$  with 2 young (2 months) and 2 old (21 months) samples. Data from GEO accession number GSE4332 (ref. 3): HSCs were defined as  $\text{Lin}^-/\text{c-Kit}^+/\text{Sca1}^+/\text{CD34}^-/\text{Flk2}^-$  with 3 young (2–3 months) and 5 old (22–24 months) samples. Results are heatmaps of expression measurements for probes mapping to *Mcm* genes with non-supervised hierarchical clustering using Euclidean distance and Ward's linkage.

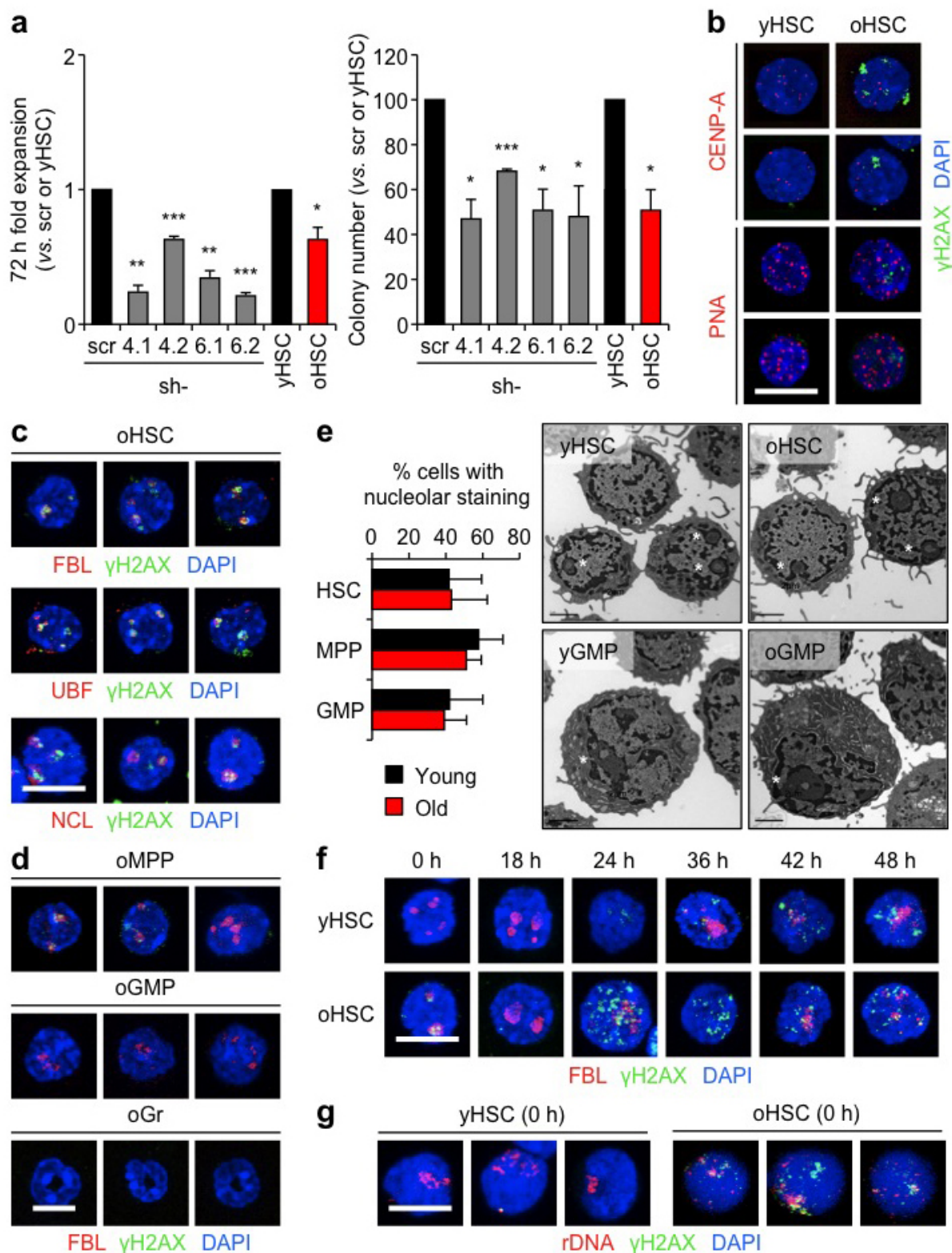




### Extended Data Figure 7 | Consequences of replication stress and decreased *Mcm* expression for HSC function.

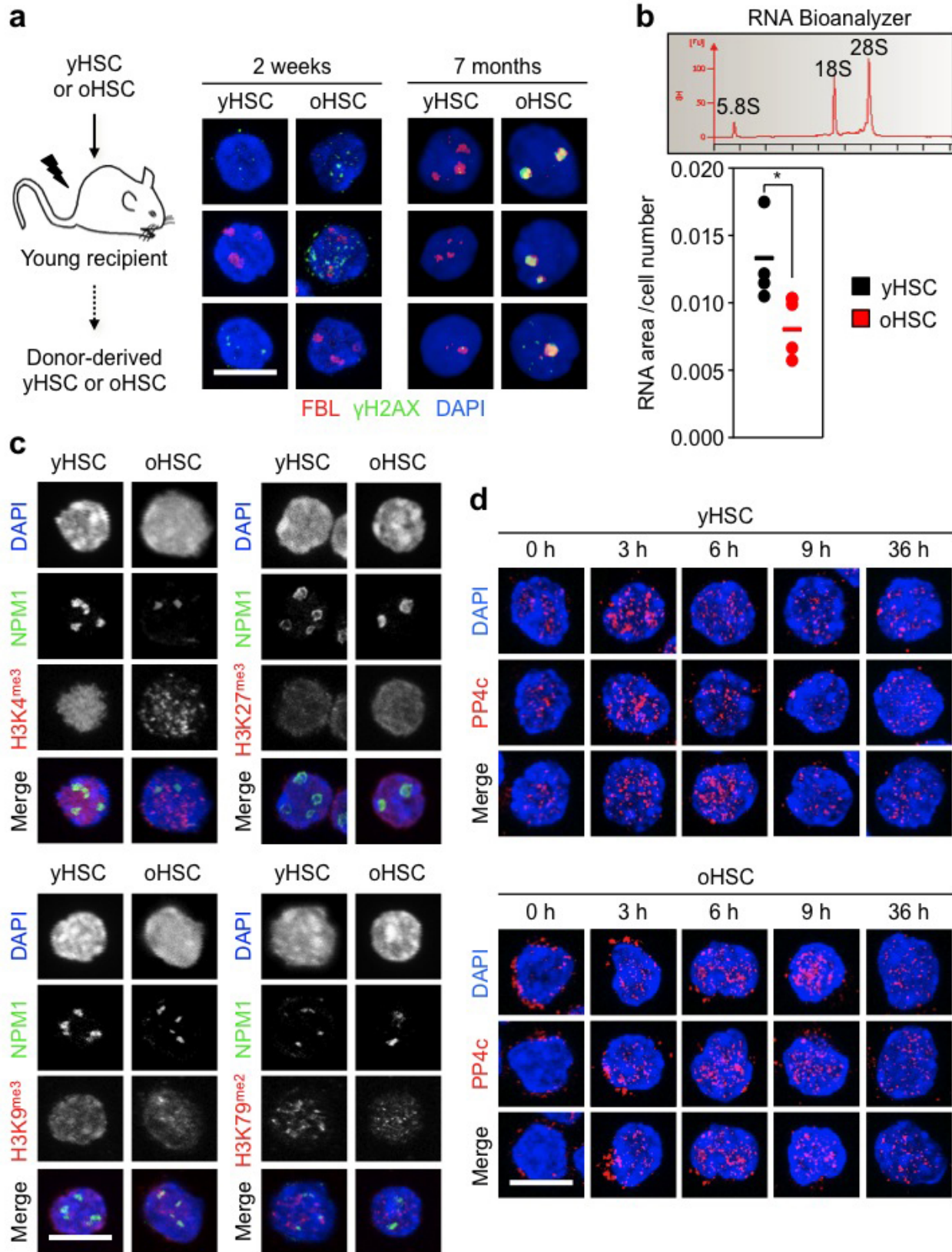
**a**, Effect of replication stress on the reconstitution ability of young and old HSCs. HSCs were isolated from C57BL/6-CD45.2 donor mice, treated with aphidicolin (Aph; 50 ng ml<sup>-1</sup>) or vehicle (Veh; DMSO) for 36 h *in vitro* and transplanted (250 HSCs per mouse) into lethally irradiated young C57BL/6-CD45.1 recipients ( $n = 5$  mice per cell type) together with 300,000 Sca1-depleted CD45.1 helper bone marrow cells. The percentage of donor-derived chimaerism and myeloid (light blue) versus lymphoid (dark blue) reconstitution in the peripheral blood was assessed by flow cytometry at the indicated months post-transplantation. Black star indicates bone marrow failure, dagger indicates animal mortality. **b**, Donor-derived chimaerism in the HSC compartment of the surviving mice at 4 months post-transplantation ( $n = 3-5$ ). **c**, Differential killing of young and old HSCs

after 72 h treatment. Eto, etoposide (0.25  $\mu$ M); HU, hydroxyurea (100  $\mu$ M); Stau, staurosporine (5 nM). Results are normalized for vehicle-treated cells and expressed as fold change compared with young HSCs (set to 1). **d**, Additional images of CldU/IdU-labelled stretched DNA fibres from replicating young and old HSCs. **e**, **f**, Effect of lentiviral-mediated knockdown of *Mcm4* and *Mcm6* on young HSCs ( $n = 3$ ): **e**, additional images for MCM4 and MCM6 protein levels (with MFI quantification) and  $\gamma$ H2AX foci; **f**, qRT-PCR analyses of *Mcm4* and *Mcm6* expression levels. Transduced GFP<sup>+</sup> HSCs were re-isolated 48 h post-infection. Results are expressed as fold change compared with scrambled shRNA (scr)-infected HSCs. Two independent shRNA constructs are used per gene. UT, untransfected. Data are means  $\pm$  s.d. \* $P \leq 0.05$ , \*\* $P \leq 0.01$ , \*\*\* $P \leq 0.001$ . NS, not significant. Scale bars, 1.5  $\mu$ m insert, 3.5  $\mu$ m (d); 10  $\mu$ m (e).



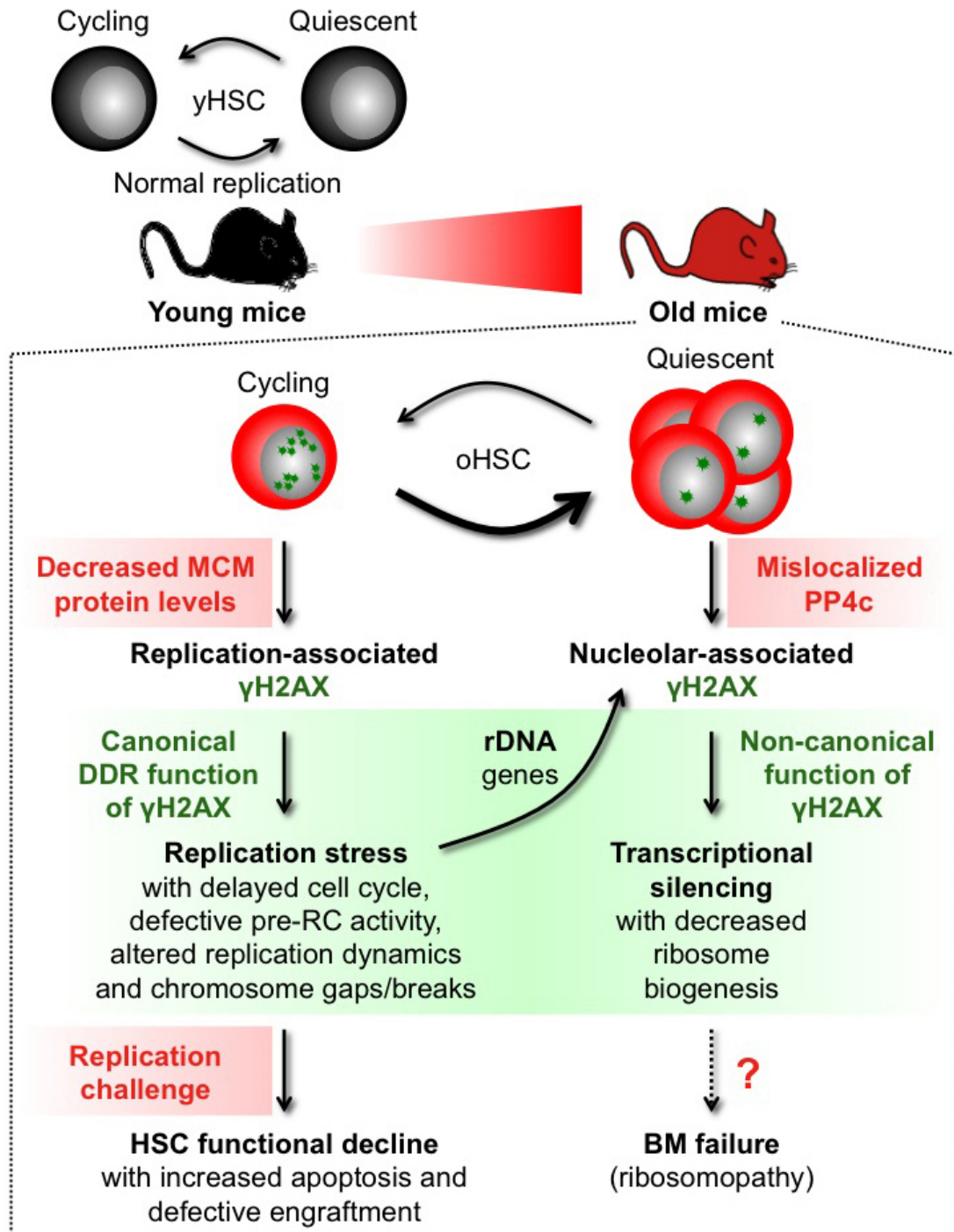
**Extended Data Figure 8 | Replication stress leads to persistence of nucleolar-associated  $\gamma$ H2AX signals in quiescent old HSCs.** **a**, Functional effect of lentiviral knockdown of *Mcm4* and *Mcm6* on young HSCs, and direct comparison with old HSCs in liquid culture expansion (left) and methylcellulose (right). Transduced GFP<sup>+</sup> HSCs were re-isolated 48 h post-infection. Results are expressed as fold change compared with scrambled shRNA (scr)-infected HSCs for transduced HSCs, and young HSCs for old HSCs. Two independent shRNA constructs are used per gene. **b**, Representative images of  $\gamma$ H2AX and centromeric marker (CENP-A) staining and immunofluorescence for  $\gamma$ H2AX and telomeric PNA probe in young and old HSCs.

**c**, Additional images for  $\gamma$ H2AX and nucleolar marker co-localization in old HSCs. **d**, Representative images of  $\gamma$ H2AX and nucleolar marker co-localization in old MPPs, GMPs and granulocytes (Gr). **e**, Percentage of young and old cells with nucleolar staining (HSC: 445 and 464; MPP: 485 and 390; GMP: 179 and 223 cells scored, respectively) and representative electron microscopy images of young and old HSCs and GMPs. Data are means  $\pm$  s.d. White asterisks indicate nucleoli. **f**, Representative images of  $\gamma$ H2AX/FBL staining in cultured young and old HSCs. **g**, Additional images of immunofluorescence for  $\gamma$ H2AX and rDNA probe in young and old HSCs. Scale bars, 10  $\mu$ m (b, c, d, f, g); 2  $\mu$ m (e).



**Extended Data Figure 9 | Decreased ribosome biogenesis and mis-localization of the PP4c phosphatase in quiescent old HSCs.** **a**, Schematic and representative images of  $\gamma$ H2AX/FBL staining in cycling and quiescent donor-derived young and old HSCs re-isolated at the indicated times after transplantation. **b**, RNA Bioanalyzer track showing the predominant 5.8S, 18S and 28S rRNA peaks, and quantification of RNA content in quiescent young

and old HSCs ( $n = 4$ ). Results are expressed as area under the curve divided by the total number of cells in each sample. Data are means  $\pm$  s.d. \* $P \leq 0.05$ . **c**, Representative images of NPM1 (nucleolar marker) and the indicated histone methylation mark in young and old HSCs. **d**, Additional images of PP4c staining in cycling young and old HSCs. Scale bars, 10  $\mu$ m.



**Extended Data Figure 10 | Model for replication stress and  $\gamma$ H2AX accumulation in old HSCs.** In contrast to HSCs isolated from young mice (yHSC), which replicate normally, HSCs isolated from old mice (oHSC) have severe replication defects due to decreased expression of mini-chromosome maintenance (MCM) DNA helicase components. Cycling old HSCs show heightened levels of replication-associated  $\gamma$ H2AX foci (small green stars) and increased levels of replication stress associated with cell cycle defects, altered DNA fork replication dynamics and chromosome gaps/breaks. Nonetheless, old HSCs usually survive replication unless confronted with a strong replication challenge such as treatment with a replication stressor drug or transplantation, which preferentially kill them and lead to their defective engraftment *in vivo*. Cycling old HSCs are also likely to accumulate  $\gamma$ H2AX foci on rDNA genes as a consequence of replication stress occurring at these hard-to-replicate loci during their replication in late S phase. However, stalled or collapsed replication forks appear to be repaired upon activation of the canonical DNA damage response (DDR), resulting in essentially undamaged rDNA genes in old HSCs. In contrast, the clearance of  $\gamma$ H2AX foci is probably unfinished by the time old

HSCs re-enter quiescence, thereby aggregating leftover  $\gamma$ H2AX signals in reformed nucleoli in post-mitotic cells. We propose that ineffective dephosphorylation of  $\gamma$ H2AX due to mislocalization of PP4c phosphatase in quiescent old HSCs contributes to the long-term persistence of nucleolar-associated  $\gamma$ H2AX signals (large green stars) in the absence of ongoing DNA damage and DDR activation. Persistent nucleolar  $\gamma$ H2AX also acts in a non-canonical manner as a histone modification marking the transcriptional silencing of rDNA genes and decreased ribosome biogenesis in quiescent old HSCs. Whether decreased rDNA transcription in quiescent old HSCs is involved in bone marrow (BM) failure syndromes associated with defective ribosome biogenesis (ribosomopathy) remains to be determined. However, as soon as old HSCs re-enter the cell cycle, PP4c is re-localized to the nucleus and quickly dephosphorylates nucleolar  $\gamma$ H2AX, thereby restoring ribosome biogenesis. Our results demonstrate that accumulation of  $\gamma$ H2AX in old HSCs marks either ongoing or residual replication stress caused by the inability of ageing HSCs to maintain normal levels of MCM proteins. They highlight the MCM DNA helicase as a potential molecular target for rejuvenation therapies.